Structural and Electrochemical Analysis of Iron Doping in LiNi_0.6-x Mn_0.2 Co_0.2 Fe_x O_2 battery

Anisa Raditya Nurohmah
Department of Chemical Engineering, Faculty of Engineering, Universitas Sebelas Maret

Cornelius Satria Yudha
Department of Chemical Engineering, Faculty of Engineering, Universitas Sebelas Maret

Mintarsih Rahmawati
Department of Chemical Engineering, Faculty of Engineering, Universitas Sebelas Maret

Shofirul Sholikhatun Nisa
Department of Chemical Engineering, Faculty of Engineering, Universitas Sebelas Maret

他

https://doi.org/10.5109/4372263

出版情報：Evergreen. 8 (1), pp.82-88, 2021-03. 九州大学グリーンテクノロジー研究教育センター
バージョン：

Structural and Electrochemical Analysis of Iron Doping in $LiNi_{0.6-x}Mn_{0.2}Co_{0.2}Fe_xO_2$ battery

Anisa Raditya Nurohmah[1], Cornelius Satria Yudha[1], Mintarsih Rahmawati[1], Sho firul Sholikhatun Nisa[1], Arif Jumari[1], Hendri Widiyandari[2], and Agus Purwanto[1,*]

[1]Department of Chemical Engineering, Faculty of Engineering, Universitas Sebelas Maret, Jl. Ir. Sutami 36 A, Surakarta, Central Java 57126, Indonesia

[2]Department of Physics, Faculty of Mathematic and Natural Science, Universitas Sebelas Maret, Jl. Ir. Suta mi 36 A, Surakarta, Central Java 57126, Indonesia

*Author to whom correspondence should be addressed:
E-mail: aguspurwanto@staff.uns.ac.id

(Received October 5, 2020; Revised March 21, 2021; accepted March 25, 2021).

Abstract: Doping in Li-ion Battery cathode material has become an interesting subject around the world. $LiNi_{0.6}Mn_{0.2}Co_{0.2}O_2$ is a high energy density cathode material. According to its ability to form particles with a high degree of atomic homogeneity, the co-precipitation method was chosen for the synthesis of the material $LiNi_{0.55}Mn_{0.2}Co_{0.2}Fe_{0.05}O_2$ (Fe-doped NMC622). In this study, Fe was used as a doping agent because of their high-energy metal oxygen bond dissociation, Oxalic acid is used as precipitant, while ammonia is used as chelating agent. Under the air stream, the oxalate precursor obtained was sintered. The characterization of the Fe-doped NMC622 is performed. Hexagonal-layered material structure shown in x-ray diffraction patterns. XRF analysis confirmed the composition of the final product. SEM (scanning electron microscope) study displayed the material's morphology. The electrochemical performance was achieved by a charge-discharge test at 1/10 C between 2-4.8 V. The Fe doped NMC622 exhibited enhancing cycle efficiency and structural characteristic compared to the un-doped NMC622.

Keywords: NMC; cathode; doping

1. Introduction

Energy is a crucial aspect for human civilization, since almost all activities rely on the availability of energy, one of which is in the transportation sector and portable devices[1)]. The use of fossil-fuel vehicles has begun to be replaced with more efficient and environmentally friendly electric cars. Energy storage in the form of electronic devices is needed to be efficient, lightweight, not over-sized, and has high performance along with its growth. Electricity is the main catalyst for urbanization , industrialization and economic development[2)].

A significant role in the lithium ion battery performance is cathode material. The cathode's structure is entirely responsible for the transfer process of lithium ions, both during lithium ions de-intercalation (charging) and lithium ions intercalation (discharging)[3)]. Lithium-ion batteries (LIBs) not only used for small but also medium-sized electricity storage systems, but the production of large-scale storage systems has been limited due to safety and economic concerns[4)].

$LiCoO_2$ (lithium cobalt oxide) is the first layer structured cathode that has been produced commercially. Since this material was deemed costly, hazardous and highly combustible when used in extreme conditions [5)], the use of this material began to reduce. With the same characteristics of operating voltage, NMC (Lithium Nickel Manganese Cobalt Oxide) has a far greater potential than $LiCoO_2$. Typically used LIB cathodes such as $LiCoO_2$. are synthesized from small mineral supplies and thus simple , low-metal-free[6)]. Based on economic considerations, NMC has a lower price than $LiCoO_2$ as Ni and Mn became replacement of cobalt. Because Co is a low natural resource, a substitute cathode material to $LiCoO_2$. is essential[7)]. NMC is a lithium battery cathode material excellent features such as high capacity, better thermal and current stability, relatively high volume density and long life cycle[8)].

Recently, research on lithium ion batteries has concentrated mainly on rising energy density and there's no reduction in life cycle and safety concerns. That is caused by the structural instability of anode and cathode chemical compounds. The instability of the active ingredient can cause thermal runaway cell batteries in an

uncontrolled exothermic reaction. Thermal runaway that caused by highly reactive oxygen released at the cathode, it is caused by phase transitions at high temperatures and flammable organic carbonate-based electrolyte reactions [9]. Therefore, the structural stability of active cathode with high energy densities such as $LiNiMnCoO_2$ (NMC) is important in order to ensure stable, high-energy cathode active materials [10].

Atomic doping is a widely used process to stabilize the cathode's chemical structure. The crystal structure can be specially modified by atomic doping which implies cation substitution in the host structure. High bond dissociation energy offers a good structural stability through structural decomposition of NMC and thus inhibits oxygen release which is an unavoidable procedure [11]. The elements for doping that have been investigated are Al [12–14], Mg [15], Ti [16], Cr [17], Mo [18], Nb [17], Sn [11] and Fe [12,19,20]. Generally, discharge capability decreases with increased concentrations of doping elements due to the presence of doped elements which are not electrochemically active [11], however, the structural stability increases [12,16,18,20,21].

NMC622 cathode materials have been known as next generation cathode materials due to their higher capacity and lower raw material costs than commercialized cathode materials such as NMC532. Many manufacturing companies have also made every attempt to commercialize and adapt the NMC622 to the lithium ion battery technology, such as the energy storage system (ESS).

Transition metals that have high dissociation energy and are quite easy to find in the interesting nature to study is Fe. Previous studies using Fe as doping element has been performed. Wilcox synthesized $Li(Ni_{0.4}Co_{0.15}Fe_{0.05}Mn_{0.4})O_2$ using combustion method in the process with glycine nitrate. Cells containing $Li(Ni_{0.4}Co_{0.15}Fe_{0.05}Mn_{0.4})O_2$ cycled to 4.3 V showed reduced efficiency relative to $Li(Ni_{0.4}Co_{0.15}Fe_{0.05}Mn_{0.4})O_2$ while iron should be electroactive in the range of operating voltages and there is no rate improvement impact [12]. Park also used Fe as doping element to synthesize $LiNi_{1/3}Co_{1/3}Mn_{1/3}Fe_x(OH)_2$ from LIB that have been used and using hydroxide co-precipitation. Fe 's positive effects on NMC 's electrochemical and thermal properties make it simpler to extract Fe from spent LIBs in leach liquors. The previous study in NMC442 and NMC111, so it can be a novelty to use Fe as a doping in NMC622 that has higher capacity and lower cost, since Indonesia is the first rank in nickel source so if we use more nickel in battery can be good advantages. Manganese and Cobalt also have some contribution in NMC, so it maintained that way.

Thus there is no research that used Fe as a doping on NMC622 batteries using co-precipitation process. Direct doping during co-precipitation is kind of method that more efficient compared to the conventional sequential doping technique.

In this study, we used batch co-precipitation method to perform NMC synthesis with iron doping ($LiNi_{0.55}Mn_{0.2}Co_{0.2}Fe_{0.05}O_2$ or Fe-doped NMC622), in an attempt to reduce the complexity of the previously mentioned current processes. Technical grade materials like Li, Ni, Mn, Co and Fe are used for co-precipitation; ammonia used as a chelating agent; and oxalic acid for a precipitation agent. As far as we consider, this approach has never been reported in previous studies. The product's electrochemical performance was tested with graphite as a commercial counter anode in a full cell cylindrical battery. The implementation on NMC and commercial NMC samples of the output values is comparable.

2. Materials and Method

2.1 Tool

The synthesize of Fe-doped NMC622 cathode have used several laboratory tools such as vacuum oven, 200 filter mesh, beaker glass, filter paper, bottle flask, measuring glass, pipette dropper, mortar and pestle, magnetic stirrer, spoon, vacuum mixing, automatic coating machine, hot rolling machine, glove box, furnace. X-Ray Diffractometer (XRD), XRF analyzer, FTIR spectrometer, and Scanning Electron Microscope (SEM) and Battery Analyzer are used for product characterization instruments.

2.2 Material

The primary materials used in the production of Fe-doped NMC622 cathode batteries are Ni_2SO_4 from Zenith (High Purity Grade), $CoSO_4$ technical grade (Rubamin, India), $FeSO_4$ (Pudak, China). Additional ingredients are Ammonia as chelating agents, oxalic acid as precipitant, AB, PVDF, KS6, LiOH S.A. 98% (Leverton, US), $LiPF_6$/EC:DEC(3:7) electrolyte, graphite anodes, PP separators.

2.3 Experimental Method

2.3.1 Synthesis $Li[Ni_{0.55}Mn_{0.2}Co_{0.2}Fe_{0.05}]O_2$ (Fe-doped NMC622)

Synthesis of $LiNi_{0.55}Mn_{0.2}Co_{0.2}Fe_{0.05}O_2$ or Fe-doped NMC622 cathode material by preparing raw materials and additives. The composition we planned is Ni 0.55, Mn 0.2, Co 0.2 and Fe 0.05, it is the modification of NMC622. The metal sulfate (Ni, Co, Mn, Fe) were diluted in distilled water to get 2 M concentration. Using a magnetic stirrer, the solution was stirred to form homogenous solution. Then ammonia and oxalic acid were added simultaneously (equimolar amount) to pH = 2 until a pale cloudy slurry is formed. The slurry was vigorously mixed while the pH and temperature of 60℃ was maintained for 2 hours. After the co-precipitation process, the precipitate is taken by passing it into the paper filter and washed until the filtrate is neutral. The precursor is dried and mixed with LiOH using mortar and pestle. LiOH is in 3% excess. Presintering is carried out at 480 ℃ for 6 hours, and 12 hours at 800 ° C sintering.

The as obtained sample was ground and sieved using 300 mesh SS-filter. Filtered powder were tested using XRF, XRD, FTIR and SEM. Then, Before the coating process NMCF sample, PVDF and AB were dried in an oven. NMC: AB: PVDF with a ratio of 92:3:5 were quickly mixed and dispersed in NMP solvent. The mixing slurry was coated on both al foil and dried for one night in the vacuum oven.

2.3.2 Fe-doped NMC622 Characterization

An XRD (X-Ray Diffractometer) from D2 Phaser Bruker, Germany, was used for the analysis of the crystal structure of the product using CuK α radiation λ =1.54 Å with 2θ range of 10–80° and a scanning rate of 0.02° per second. A scanning electron microscope (SEM) (JEOL JSM-6510LA, Japan) was used in the morphs of the sample. The substances Ni, Mn , Co and Fe were analyzed using X-Ray Fluorescence (Bruker XRF Spectrometer, Germany) in powder form. Fourier Transformed Infrared Spectroscopy (Shimadzu FTIR spectrometer, Japan) was used for analyzed the functional groups and surface composition of the material. Depending on the characterization result, the best possible synthesis material continued battery performance testing in cylindrical cell battery using a NEWARE Battery Analyzer and BTS program with a voltage window of 2.5–4.3 V at 0.1 C or 20 mA/g (1 $C_{theoretical}$ = 200 mAh / g).

3. Result and Discussion

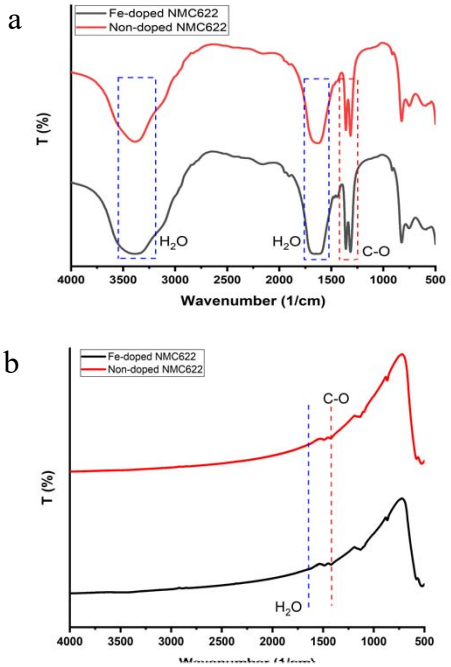

Fig. 1 : FTIR spectra Fe-doped NMC622 Precursor (a) and Fe-doped NMC622 Product (b)

The synthesis of Fe-doped NMC622 materials is achieved by a process of co-precipitation. At precipitation, oxalic acid is used as precipitant and as chelating agents was using ammonia to control the coagulation process on the NMC cathode.

Fig. 1a shows the absorbance spectrum of the Fe-doped NMC622 and Non-doped NMC622 precursors The same pattern has shown The bending vibration of the water molecule can be seen from the big peak around 3340cm^{-1} and 1600cm^{-1}. The sharp peaks located at around 1300cm^{-1} correlate to the Carbon-Oxygen bond. Overall, the sample's infrared absorbance spectrum is same as $FeC_2O_4.2H_2O$, which indicates that the precipitation of NMC-oxalate occurs with the reaction referred to in equation 1-2. After adding excess lithium, the precursors are prepared for sintering. In sintering, the Hydrogen-Oxygen-Hydrogen and the Carbon-Oxygen bonds are lost. This could be used to answer that by sintering shows the loss of bonds at the precursors as shown in Fig. 1b [22].

$$xNi^{2+}_{(aq)} + yMn^{2+}_{(aq)} + zCo^{2+}_{(aq)} + NH_4OH_{(aq)} \rightleftharpoons Ni_xMn_yCo_z(NH_3)^{2+}_{(aq)} + H_2O_{(l)} \quad (1)$$

$$Ni_xMn_yCo_z(NH_3)^{2+}_{(aq)} + H_2C_2O_{4(aq)} \rightarrow Ni_xMn_yCo_zC_2O_4 \downarrow_{(s)} + NH_4^+{}_{(aq)} \quad (2)$$

An XRF study has confirmed the composition of active cathode synthesized materials. The sample formed for Fe-doped NMC622 is 59.94 % Ni, 16.53 % Mn, 18.64 % Co, and 4.89 % Fe, as shown in Table 1. The sample formed for non-doped NMC622 is 59.09 % Ni, 19.89 % Mn, and 21 % Co. The compositions are significantly lower than originally planned values and lithium composition has been set as a mole ratio of 1.03 for transition metals in active cathode materials. It is clearly seen that the composition of Ni is 59.94% among quarternary metals, which is close to the target value of 55%, while the composition of Mn and Co is 16.53% and 18.64% respectively, which is less related to the target value of 20%, and the composition of Fe atoms is 4.89%, which is close to the target value of 5%.. Based on Patnaik[23], K_{sp} value of Ni, Co, Mn and Fe hydroxide is 2.0 x 10^{-15}, 1.9 x 10^{-13}, 1.6 x 10^{-15}, and 8.0 x 10^{-16} respectively. When compared to Ni, Co and Fe, Mn faced the most concentration depreciation. Since Mn has the highest Ksp value (solubility product) relative to the Ksp value of Ni and Co, so that the deposition yield from Mn is lower[24]. Fe concentration is the closest to target value because it has the lowest solubility, so the precipitation process show more effective.

Table 1. Molar fraction of ternary metal of Fe-doped NMC622 and non-doped NMC622

Sample	Element			
	Ni (%)	Mn(%)	Co(%)	Fe(%)
Fe-doped NMC622	59.94	16.53	18.64	4.89
Non-doped NMC622	59.90	19.89	21.10	-

Fig. 2 shown X-ray diffraction patterns of Fe-doped NMC622 and non-doped NMC622 powder. With group space R3 m (No. 166) [25], the pattern reflexes indexed to the α -NaFeO2-like hexagonal structure. The reflexes obtained at 38° and 65° 2θ in (006)/(102) and (108)/(110) show well crystallized materials [26].

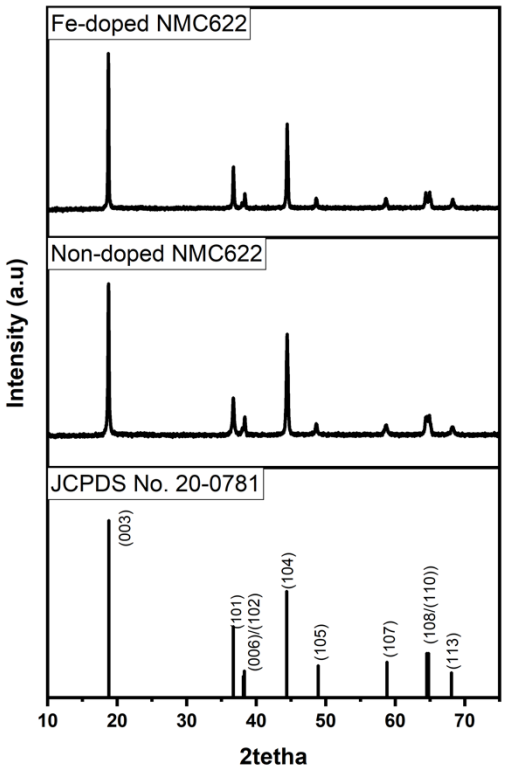

Fig. 2 XRD analysis of Fe-doped NMC622

Table 2 lattice parameters of samples with Fe doping and pure

Sample	a	c	c/a	I003/I104
Fe-doped NMC622	2.868	14.285	4.979	1.622599
Non-doped NMC622	2.870	14.142	4.927	1.370756

Ni^{2+} may have a bad effect on the performance of Fe-doped NMC622 cathode material during phase formation, mostly because of the close radii, Li atomic radii replacing Li with Ni^{2+}. A stable Ni^{2+} ion blocking the Li-ion pathway is very difficult to oxidize, inhibits its intercalation and de-intercalation process which results in low electrochemical efficiency. It is called by cation mixing, and the intensity ratio of I(003)/I(104) evaluation may indicate its degree or level [27]. I(003)/I(104) intensity ratio is normally used to specify the level of cation mixing in the Li-layers [28]. If the value of I(003)/I(104) is higher than 1.2, cation mixing is considered poor and normally the layered structure is perfect. I(003)/I(104) intensity ratio value in the Fe-doped material is 1.622 and non-doped material is 1.37, indicating a lower cation mixing. Lattice parameters of Fe-doped NMC622 and non-doped NMC622 shown in Table *2*. The lattice expansion was slightly increased in the presence of Fe doping, which indicates that the Fe^{2+} ion had been doped into the Li ($Ni_{0.6}Co_{0.2}Mn_{0.2}$) O2 lattice during the calcination process. Because metal ions, for example, Ni^{2+} (0.069 nm), Co^{3+} (0.0545 nm), and Mn^{4+} (0.054 nm), have smaller ionic radii than Fe2 +, when replaced by Fe^{2+} ions (0.076 nm), Fe^{2+} will enlarge the lattice parameter. This is also the same as that done by previous studies with Mg and Zn doping[29].

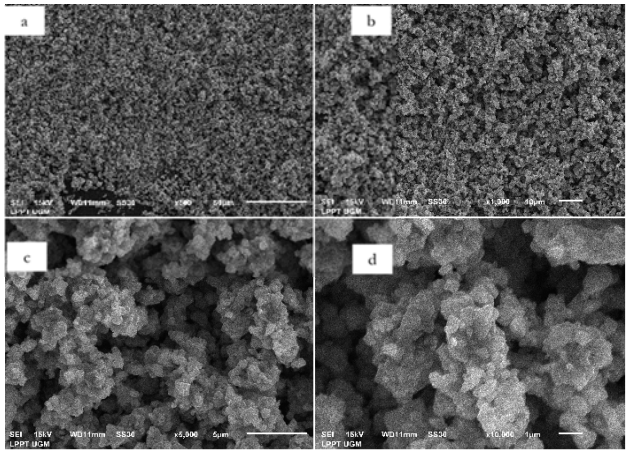

Fig. 3 SEM images of Fe-doped NMC622 (a) at 500 x magnification, (b) at 1000 x magnification, (c) at 5000 x magnification, (d) at 10,000 magnification

Fig. 3 Presents the synthesized Fe-doped NMC622 particles at various magnification. Based on the SEM images, the product has an average primary particle size of 0.509 micrometers with the range of 0.203-1.015 micrometers. Based on Fig. 3d, size of the secondary polyhedral shaped particles is approximately 1.35-6.09 micrometers and the average size of the secondary particles is 3.47 micrometers. Secondary particle is the agglomerate of the primary particle. Using Fe as doped metal in NMC622 have made smaller primary particle size.

The NMC622 sample with Fe doping has an average size that is relatively smaller than that of previous studies using the co-precipitation method on non-doped material[30], which, as previously reported, could be caused by Fe doped which may reduce particle size [31]. Smaller particles however have advantages, as well as larger surface area and faster lithium ion transfer rather than larger particles [27].

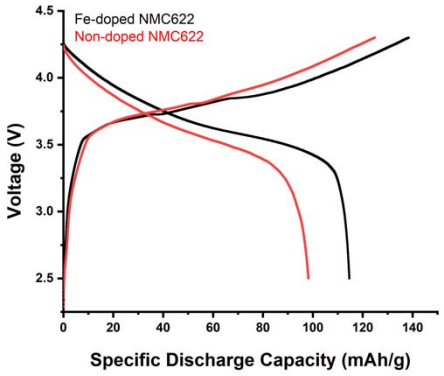

Fig. 5 Charge-discharge analysis of Fe-doped NMC622

Fig. 4 demonstrates the charge and discharge of the as-prepared Fe-doped NMC622 and non-doped NMC622 under ambient conditions in a range of voltage 2.5 V-4.3 V using 0.1 C current. The first charge of the as-prepared Fe-doped NMC622 and non-doped NMC622 was resulted a charge capacity of 140 mAh/g and 125mAh/g followed by its first 114.59 mAh/g and 98.33 mAh/g discharge capacity, respectively. Theoretical battery capacity for NMC is 200 mAh/g. Previous study by Park, NMC333 with added 5% Fe have discharge capacity 162.0 mAh/g [20]. In the case of fe-doping, the primary explanation for lower discharge capacity in Ni-rich materials is due to increased Li-diffusion hindrance and increased oxidation capability of the Fe ions [32,33]. However, because the structure of the cathode, depending on the re-conversion reaction, varies during each charging and discharge process, the efficiency of the cathode depends significantly on the different treatments, such as the mixing of electrode materials, the current rate and the temperature[34].

The cycle performance of the active cathode material in range of voltage 2.5 and 4.3 V at a constant current density of 90 mA/g (0.2*C*) shown in Fig. 5. a shows the performance of the Fe-doped NMC622 and Non-doped NMC622 cycles. The normalized capacity in b is the actual capacity, the initial capacity, of each sample. Fe-doped NMC622 and non-doped NMC622 have different cycling behaviour for 50 cycles at a rate of 0.2 C and have a retention rate of 85.76 % and 62.84 %. Capacity decline occurred during the initial cycles; however, after three to four cycles, capacity is considered stable after 50 cycles for Fe-doped NMC622. But NMC without doping has lower capacity retention and poor stability. In addition, Fe doping obtained the structural stability required for improved cycling [35]. shows that the Fe doped NMC622 has a stable coulombic efficiency. The performance capacity of the battery cell at various charging / discharge rates has been calculated in order to check the efficiency of the battery[36].

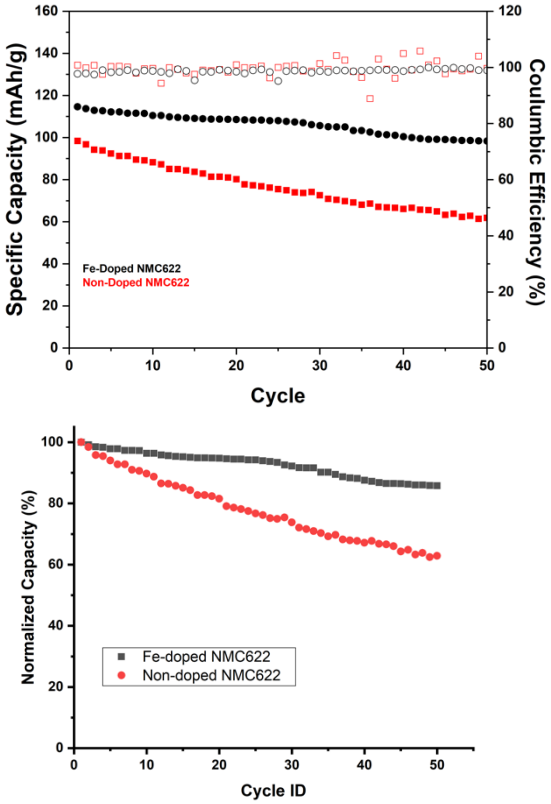

Fig. 4 Cycling performance (discharge capacity and coulombic efficiency) and (b) the normalized cycle performance of Fe-doped NMC622 and Non-doped NMC622 at 0.2C

4. Conclusion

The NMC622 cathode which was doped with Fe has been successfully synthesized using direct co-precipitation process and studied about the electrochemical performance and structural effects of doping. Structural studies show dopants have an effect on particle size. The initial discharge capacity of Fe-doped NMC622 and non-doped NMC622 is 114.59 and 98.33 mAh/g, respectively, while the retention capacity at 0.2 C' for 50 cycles is 85.76 % and 62.84 % respectively. The results show for certain if Fe doping can improve the stability of NMC622. However, future developments in the optimization of process variables are needed in order to obtain better material. Further work is required in the future to obtain a better and more reliable discharge capacity.

Acknowledgements

This paper is supported by Indonesia Endowment Fund for Education (Lembaga Pengelola Dana Pendidikan/ LPDP) through Pendanaan Riset Inovatif Produk (Rispro) Invitasi grant no.PRJ-6/LPDP/2020. This paper is also supported by PT Pertamina with contract number 007/P00000/2019-S0.

References

1) B. Xie, A. Kitajou, S. Okada, W. Kobayashi, M. Okada, and T. Takahara, "Cathode properties of na3mpo4co3 (m = co/ni) prepared by a hydrothermal method for na-ion batteries," *Evergreen*, **6** (*4*) 262–266 (2019). doi:10.5109/2547345.
2) K. Marzia, M.F. Hasan, T. Miyazaki, B.B. Saha, and S. Koyama, "Key factors of solar energy progress in bangladesh until 2017," *Evergreen*, **5** (*2*) 78–85 (2018). doi:10.5109/1936220.
3) N. Nitta, F. Wu, J.T. Lee, and G. Yushin, "Li-ion battery materials: present and future," *Mater. Today*, **18** (*5*) 252–264 (2015). doi:10.1016/j.mattod.2014.10.040.
4) K. Nakamoto, R. Sakamoto, A. Kitajou, M. Ito, and S. Okada, "Cathode properties of sodium manganese hexacyanoferrate in aqueous electrolyte," *Evergreen*, **4** (*1*) 6–9 (2017). doi:10.5109/1808305.
5) J.R. Dahn, E.W. Fuller, M. Obrovac, and U. von Sacken, "Thermal stability of lixcoo2, lixnio2 and λ-mno2 and consequences for the safety of li-ion cells," *Solid State Ionics*, **69** (*3–4*) 265–270 (1994). doi:10.1016/0167-2738(94)90415-4.
6) K. Chihara, M. Ito, A. Kitajou, and S. Okada, "Cathode property of na2cxox [x = 4, 5, and 6] and k2c6o6 for sodium-ion batteries," *Evergreen*, **4** (*1*) 1–5 (2017). doi:10.5109/1808304.
7) A. Nojima, A. Sano, H. Kitamura, and S. Okada, "Electrochemical characterization, structural evolution, and thermal stability of livopo4 over multiple lithium intercalations," *Evergreen*, **6** (*4*) 267–274 (2019). doi:10.5109/2547346.
8) D. Doughty, and E.P. Roth, "A general discussion of li ion battery safety," *Electrochem. Soc. Interface*, **21** (*2*) 37–44 (2012). doi:10.1149/2.F03122if.
9) S. Hildebrand, C. Vollmer, M. Winter, and F.M. Schappacher, "Al2O3, sio2 and tio2 as coatings for safer lini0.8co0.15al0.05o2 cathodes: electrochemical performance and thermal analysis by accelerating rate calorimetry," *J. Electrochem. Soc.*, **164** (*9*) A2190–A2198 (2017). doi:10.1149/2.0071712jes.
10) H.J. Noh, S. Youn, C.S. Yoon, and Y.K. Sun, "Comparison of the structural and electrochemical properties of layered li[nixcoymnz]o2 (x = 1/3, 0.5, 0.6, 0.7, 0.8 and 0.85) cathode material for lithium-ion batteries," *J. Power Sources*, **233** 121–130 (2013). doi:10.1016/j.jpowsour.2013.01.063.
11) M. Eilers-Rethwisch, M. Winter, and F.M. Schappacher, "Synthesis, electrochemical investigation and structural analysis of doped li[ni 0.6 mn 0.2 co 0.2-x m x]o 2 (x = 0, 0.05; m = al, fe, sn) cathode materials," *J. Power Sources*, **387** (*January*) 101–107 (2018). doi:10.1016/j.jpowsour.2018.02.080.
12) J.D. Wilcox, E.E. Rodriguez, and M.M. Doeff, "The impact of aluminum and iron substitution on the structure and electrochemistry of li (ni0.4 co0.2-y my mn0.4)o2 materials," *J. Electrochem. Soc.*, **156** (*12*) 1011–1018 (2009). doi:10.1149/1.3237100.
13) M. Iftekhar, N.E. Drewett, A.R. Armstrong, D. Hesp, F. Braga, S. Ahmed, and L.J. Hardwick, "Characterization of aluminum doped lithium-manganese rich composites for higher rate lithium-ion cathodes," *J. Electrochem. Soc.*, **161** (*14*) A2119–A2116 (2014). doi:10.1149/2.0441414jes.
14) M. Dixit, B. Markovsky, D. Aurbach, and D.T. Major, "Unraveling the effects of al doping on the electrochemical properties of lini0.5co0.2mn0.3o2using first principles," *J. Electrochem. Soc.*, **164** (*1*) A6359–A6365 (2017). doi:10.1149/2.0561701jes.
15) Y.X. Wang, K.H. Shang, W. He, X.P. Ai, Y.L. Cao, and H.X. Yang, "Magnesium-doped li<inf>1.2</inf>[co<inf>0.13</inf>ni<inf>0.13</inf>mn<inf>0.54</inf>]o<inf>2</inf> for lithium-ion battery cathode with enhanced cycling stability and rate capability," *ACS Appl. Mater. Interfaces*, **7** (*23*) 13014–13021 (2015). doi:10.1021/acsami.5b03125.
16) W. Cho, J.H. Song, K.W. Lee, M.W. Lee, H. Kim, J.S. Yu, Y.J. Kim, and K.J. Kim, "Improved particle hardness of ti-doped lini1/3co1/3mn1/3-xtixo2 as high-voltage cathode material for lithium-ion batteries," *J. Phys. Chem. Solids*, **123** (*August*) 271–278 (2018). doi:10.1016/j.jpcs.2018.08.008.
17) J. Mao, K. Dai, M. Xuan, G. Shao, R. Qiao, W. Yang, V.S. Battaglia, and G. Liu, "Effect of chromium and niobium doping on the morphology and electrochemical performance of high-voltage spinel lini0.5mn1.5o4 cathode material," *ACS Appl. Mater. Interfaces*, **8** (*14*) 9116–9124 (2016). doi:10.1021/acsami.6b00877.
18) B. Pişkin, C. Savaş Uygur, and M.K. Aydınol, "Mo doping of layered li (nixmnyco1-x-y-zmz)o2 cathode materials for lithium-ion batteries," *Int. J. Energy Res.*, **42** (*12*) 3888–3898 (2018). doi:10.1002/er.4121.
19) X. Cheng, H. Wei, W. Hao, H. Li, H. Si, S. An, W. Zhu, G. Jia, and X. Qiu, "A cobalt-free li(li 0.16 ni 0.19 fe 0.18 mn 0.46)o 2 cathode for lithium-ion batteries with anionic redox reactions," *ChemSusChem*, **12** (*6*) 1162–1168 (2019). doi:10.1002/cssc.201802436.
20) S. Park, D. Kim, H. Ku, M. Jo, S. Kim, J. Song, J. Yu, and K. Kwon, "The effect of fe as an impurity element for sustainable resynthesis of li[ni1/3co1/3mn1/3]o2 cathode material from spent lithium-ion batteries," *Electrochim. Acta*, **296** 814–822 (2019). doi:10.1016/j.electacta.2018.11.001.
21) H. Li, H. Guo, Z. Wang, J. Wang, X. Li, N. Chen, and W. Gui, "Improving rate capability and decelerating voltage decay of li-rich layered oxide cathodes by chromium doping," *Int. J. Hydrogen Energy*, **43** (*24*) 11109–11119 (2018).

doi:10.1016/j.ijhydene.2018.04.203.

22) A. Jumari, K. Nur, R. Stulasti, R.N. Halimah, L.A. Aini, and R. Mintarsih, "Production of lini0.6mn0.2co0.2.2o2 via fast oxalate precipitation for li-ion," *AIP Conf. Proc.*, **030011** (*April*) 2–7 (2020). doi:https://doi.org/10.1063/5.0000646.

23)P. Patnaik, "Dean's Analytical Chemistry Handbook," 2nd ed., McGraw-Hill Companies, Inc., 2004.

24) H. Widiyandari, R. Ardiansah, A.S. Wijareni, M. Yunianto, and A. Purwanto, "Synthesis of lithium nickel manganese cobalt as cathode material for li-ion battery using difference precipitant agent by coprecipitation method," *AIP Conf. Proc.*, **030023** (*2217*) (2020).

25) Y.S. Meng, G. Ceder, C.P. Grey, W.S. Yoon, and Y. Shao-Horn, "Understanding the crystal structure of layered lini 0.5mn 0.5o 2 by electron diffraction and powder diffraction simulation," *Electrochem. Solid-State Lett.*, **7** (*6*) 155–158 (2004). doi:10.1149/1.1718211.

26) M. Eilers-Rethwisch, S. Hildebrand, M. Evertz, L. Ibing, T. Dagger, M. Winter, and F.M. Schappacher, "Comparative study of sn-doped li[ni0.6mn0.2co0.2-xsnx]o2 cathode active materials (x = 0-0.5) for lithium ion batteries regarding electrochemical performance and structural stability," *J. Power Sources*, **397** (*January*) 68–78 (2018). doi:10.1016/j.jpowsour.2018.06.072.

27) C.S. Yudha, S.U. Muzayanha, H. Widiyandari, F. Iskandar, W. Sutopo, and A. Purwanto, "Synthesis of lini0.85co0.14al0.01o2 cathode material and its performance in an nca / graphite full-battery," *Energies*, **12** 1886 (2019).

28) H.Z. Zhang, Q.Q. Qiao, G.R. Li, S.H. Ye, and X.P. Gao, "Surface nitridation of li-rich layered li(li0.17ni 0.25mn0.58)o2 oxide as cathode material for lithium-ion battery," *J. Mater. Chem.*, **22** (*26*) 13104–13109 (2012). doi:10.1039/c2jm30989k.

29) H. Du, Y. Zheng, Z. Dou, and H. Zhan, "Zn-doped lini1/3co1/3mn1/3o2 composite as cathode material for lithium ion battery : preparation , characterization , and electrochemical properties," *Jounal Nanomater.*, **2015** (*Cv*) 1–6 (2015).

30) Y. Cui, K. Liu, J. Man, J. Cui, H. Zhang, W. Zhao, and J. Sun, "Preparation of ultra-stable li[ni0.6co0.2mn0.2]o2 cathode material with a continuous hydroxide co-precipitation method," *J. Alloys Compd.*, **793** 77–85 (2019). doi:10.1016/j.jallcom.2019.04.123.

31) H. Li, G. Chen, B. Zhang, and J. Xu, "Advanced electrochemical performance of li[ni(1/3-x)fexco1/3mn1/3]o2 as cathode materials for lithium-ion battery," *Solid State Commun.*, **146** (*3–4*) 115–120 (2008). doi:10.1016/j.ssc.2008.02.006.

32) G. Prado, A. Rougier, L. Fournès, and C. Delmas, "Electrochemical behavior of iron-substituted lithium nickelate," *J. Electrochem. Soc.*, **147** (*8*) 2880 (2000). doi:10.1149/1.1393620.

33) J.N. Reimers, E. Rossen, C.D. Jones, and J.R. Dahn, "Structure and electrochemistry of lixfeyni1-yo2," *Solid State Ionics*, **61** (*4*) 335–344 (1993). doi:10.1016/0167-2738(93)90401-N.

34) K. Hashizaki, S. Dobashi, S. Okada, T. Hirai, J.I. Yamaki, and Z. Ogumi, "Charge-discharge characteristics of li/cucl2 batteries with lipf6/methyl difluoroacetate electrolyte," *Evergreen*, **6** (*1*) 1–8 (2019). doi:10.5109/2320995.

35) U. Nisar, R. Amin, A. Shakoor, R. Essehli, S. Al-Qaradawi, R. Kahraman, and I. Belharouak, "Synthesis and electrochemical characterization of cr-doped lithium-rich li1.2ni0.16mn0.56co0.08-xcrxo2 cathodes," *Emergent Mater.*, **1** (*3–4*) 155–164 (2018). doi:10.1007/s42247-018-0014-0.

36) E.R. Dyartanti, I.N. Widiasa, A. Purwanto, and H. Susanto, "Nanocomposite polymer electrolytes in pvdf/zno membranes modified with pvp for use in lifepo4 batteries," *Evergreen*, **5** (*2*) 19–25 (2018). doi:10.5109/1936213.